SOILS AND FOUNDATIONS Vol. 48, No. 6, 851–857, Dec. 2008
Japanese Geotechnical Society

UNDRAINED CYCLIC SHEAR BEHAVIOUR OF RECONSTITUTED SCORIA DEPOSIT

YANYAN AGUSTIAN[i] and SATOSHI GOTO[ii]

ABSTRACT

Since scoria can be utilized in several industrial applications and the cyclic shear characteristics of scoria have not been studied sufficiently, it is important to measure the cyclic triaxial shearing response of scoria deposit. A series of laboratory tests was carried out in order to obtain the cyclic shear characteristics of scoria. Undrained cyclic triaxial tests were conducted on reconstituted scoria deposits obtained from Mt. Fuji, Yamanashi Prefecture. To evaluate the degree of particle breakage due to shearing, the grain size distribution has been evaluated before and after cyclic triaxial tests by traditional techniques. The differences in liquefaction characteristics between Scoria and other materials from previous studies were demonstrated. From the results of undrained cyclic triaxial test on the scoria, it was understood that the effect of relative density D_r on the cyclic shear strength of scoria material is small, in the range 43.8% to 97.7% of D_r. Comparison results between monotonic and cyclic triaxial tests on grain breakage due to shearing shows that the degree of grain breakage for cyclic triaxial test is relatively higher than from monotonic tests for a similar dry density.

Key words: cyclic shear strength, grain breakage, scoria, triaxial test (**IGC**: D6)

INTRODUCTION

Scoria deposits occur extensively around many volcanoes of Quarternary epoch. The characteristic of scoria aggregate is its looseness, which is encountered in industrial conditions, such as scoria storage. Scoria can be utilized in several industrial applications including the manufacturing of lightweight concrete, masonry and for insulating purposes (Sabtan and Shehata, 2000). In addition to other uses such as low cost fillers, filter materials, and absorbents scoria can be used for base in road construction as sub-base material (Hossain, 2006).

The objective of this paper is to present the laboratory test of the cyclic shear strength of reconstituted scoria sampled from Mt. Fuji and to compare the results with those of ordinary sand from the previous studies. Some studies have been concerned with the physical properties of scoria. However, only a few studies have been presented which discuss its undrained cyclic shear strength. A previous study by Kusakabe et al. (1991) shows the behaviour of undisturbed scoria in a large triaxial compression test. They concluded that the behaviour of scoria changes from a dilatant brittle material to a plastic material in 700 ~ 1500 kPa of confining pressure range, exhibiting volume reduction with particle crushing. Agustian and Goto (2008) found that at low confining stress, the dependency of internal friction of dry scoria ϕ_d on effective confining stress σ'_c in triaxial compression are considered negligible for the range of $\sigma'_c = 10 \sim 80$ kPa for all various grain sizes, with a significant dependency of grain breakage on the stress level. Hatanaka et al. (1985) investigated the undrained cyclic shear behaviour of volcanic soil, termed "shirasu", on undisturbed and reconstituted samples and found that compared with undisturbed samples, the liquefaction resistance of reconstituted samples, which had about the same density, was about 45 to 50% of the value for undisturbed samples. Miura et al. (2003) have clarified the effect of particle crushing and fabric anisotropy on the static and cyclic deformation-strength properties for volcanic coarse-grained soils.

TRIAXIAL COMPRESSION BEHAVIOUR OF SCORIA

The strength and deformation characteristics of scoria have been studied in triaxial compression tests (Agustian and Goto, 2008). While the data was limited, this experimental study has helped to explain the behaviour of dry scoria aggregates sheared at low confining stresses (10 to 80 kPa) in drained conditions. The results show that there was no striking difference in shear strength behaviour from Toyoura sand reported by Fukushima and Tatsuoka (1984). The effects of maximum grain size on

[i] Graduate Student, Interdisciplinary Graduate School of Medicine and Engineering, Natural, Biotic and Social Environment Engineering, University of Yamanashi, Japan.
[ii] Associate Professor, ditto (goto@yamanashi.ac.jp).
The manuscript for this paper was received for review on May 7, 2008; approved on October 3, 2008.
Written discussions on this paper should be submitted before July 1, 2009 to the Japanese Geotechnical Society, 4-38-2, Sengoku, Bunkyo-ku, Tokyo 112-0011, Japan. Upon request the closing date may be extended one month.

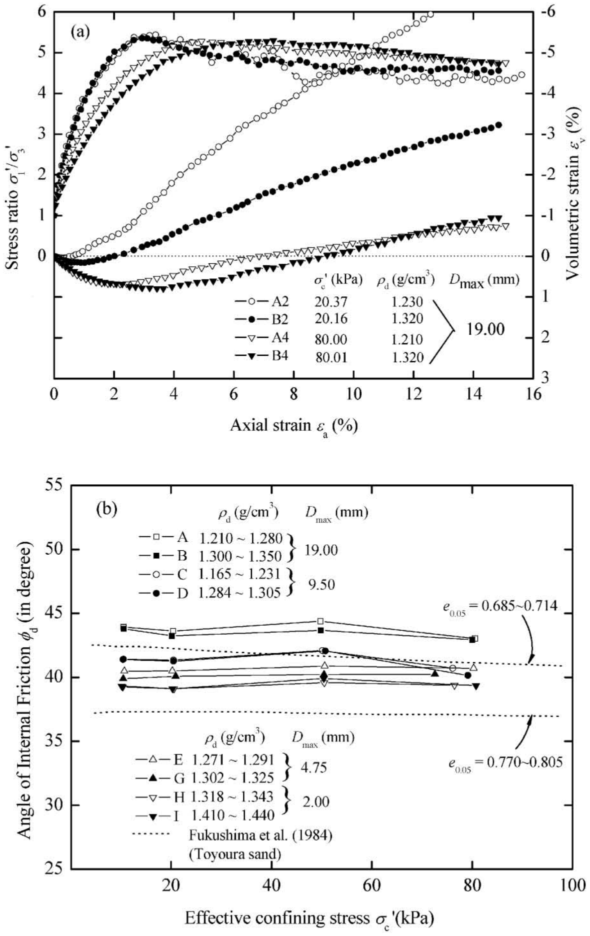

Fig. 1. Results from triaxial compression test (Agustian and Goto, 2008): (a) Relationships between stress rato, axial strain and volumetric strain of dry scoria with $D_{max} = 19.00$ mm and (b) Relationship between angle of internal friction ϕ_d and effective confining stress σ_c' of scoria in triaxial compression test

shear strength behaviour and on grain breakage have been evaluated. While the dependency of shear strength of scoria on confining stress at level 10 to 80 kPa is not significant, maximum grain size and gradation should be taken into account in evaluating the shear strength behaviour of scoria.

Figure 1 shows the test results from triaxial compression. Figure 1(a) depicts the relationships between stress ratio, axial strain and volumetric strain of dry scoria with $D_{max} = 19.00$ mm and Fig. 1(b) shows the relationships between the angle of internal friction ϕ_d and effective confining stress σ_c' from the triaxial compression tests on reconstituted specimens of scoria on various grain sizes. The results show that the dependency of ϕ_d on σ_c' are considered negligible for the range of $\sigma_c' = 10 \sim 80$ kPa for various grain sizes. The dependency is very small if any, and these are for larger grain size, say $D_{max} = 19.00$ mm and 9.50 mm, at stress level of $\sigma_c' = 50 \sim 80$ kPa. It may be due to grain breakage of scoria particles and since larger grain size of scoria particles exhibit higher crushability than smaller one.

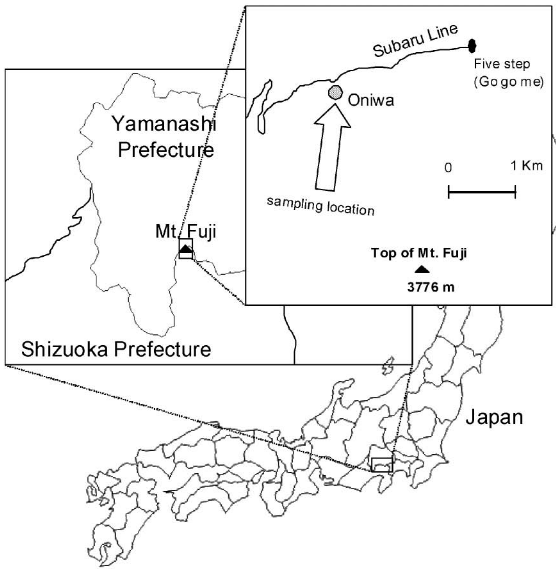

Fig. 2. Location of sampling site

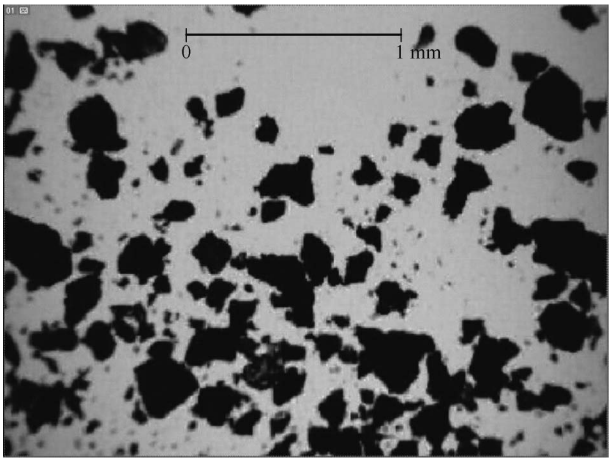

Photo 1. Photograph of scoria aggregate used in this study

MATERIAL AND TESTING PROCEDURE

The tests were carried out on scoria sampled from Mt. Fuji, Yamanashi Prefecture (Fig. 2). The scoria was washed and passed through a 2 mm sieve; with particle size in the range of 2 mm to 75 μm. Photo 1 shows the scoria aggregate enlarged 20 times using a microscope. The physical properties of scoria and the test results are shown in Table 1. The maximum and minimum void ratios of scoria were measured by using Japanese standard method.

Specimens were prepared for the tests by pluviating air dried particles through air. A pluviation apparatus was set up so that during the particles falling into mould, the scoria container was moved upwards to keep the drop height between the container and the mould constant. Densification of the samples was accomplished by increasing the pluviation height. This method leads to the formation of inherent anisotrophy in the specimens with the bedding plane being in the horizontal direction.

Table 1. Summary of test conditions and the test results

(1) Test Code	(2) B	(3) ρ_d (g/cm^3)	(4) D_r (%)	(5) R	(6) N_c	(7) B_g (%)
S01	0.99	1.25	49.80	0.21	5.10	10.21
S02	0.96	1.23	43.55	0.19	9.37	9.58
S03	0.97	1.24	47.40	0.17	14.46	6.50
S04	0.97	1.24	46.81	0.16	17.05	9.18
S05	0.97	1.24	46.72	0.14	25.18	7.75
S06	0.96	1.25	49.50	0.13	33.05	6.09
S11	0.96	1.37	92.45	0.23	6.00	17.47
S12	0.96	1.38	97.65	0.19	11.13	12.49
S13	0.96	1.37	94.31	0.16	25.51	13.76
S14	0.96	1.38	96.75	0.14	46.00	11.86

(2) Skempton's B value
(3) dry density
(4) relative density
(5) cyclic stress ratio
(6) number of loading cycles
(7) grain breakage calculated based on Marshal's method

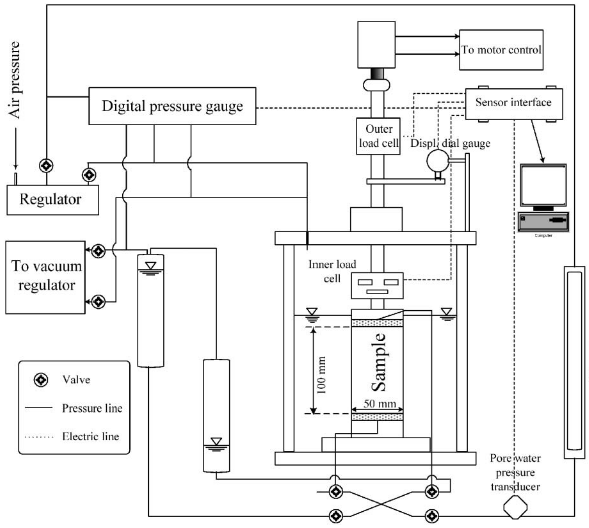

Fig. 3. Schematic diagram of cyclic triaxial in the present study

The test apparatus consists of a triaxial cell, cell pressure and back pressure control devices, an axial load control device and a data acquisition and recording system for the axial load, axial displacement, and pore water pressure of the specimen. Figure 3 is the schematic diagram of cyclic triaxial used in the present study. After obtaining the self-sustaining sample by applying 30 kPa of vacuum to the sample interior, a cylindrical chamber and the cell cover were set up and water was then poured to fill the cell water. In order to get a high degree of saturation, both the cell and sample interior were vacuumed in such a way that the confining stress is constant (30 kPa) during the process. After reaching the final stage of this process (−60 kPa for cell pressure and −90 kPa for interior sample) deaired water was circulated into the specimen for about 3 hours and then the pressure of sample interior and cell pressure were returned to −30 kPa and 0 kPa. Back pressure was then increased step by step until it reached 100 kPa and at the same time 130 kPa was applied to the cell so that the confining stress was still held at 30 kPa of constant stress. To ensure the saturation of the specimen, the degree of saturation was evaluated at this stage. The degree of saturation of specimens was evaluated by their B-value, which is defined as the ratio of pore water pressure increment to isotropic stress increment under undrained condition. By this procedure, the test was continued until B-value of the specimen was equal to or greater than 0.96. The specimen then was consolidated isotropically for 2–3 hours under confining pressure $\sigma'_c = 30 \sim 100$ kPa.

In order to examine the liquefaction strength, all the undrained cyclic tests were performed by applying uniform sinusoidal cycles of deviator stresses at a frequency of 0.05 Hz under constant cell pressure. The axial loading frequency used by previous researchers on Toyoura sand were 0.1 Hz (Hyodo et al., 1998) and 0.05 Hz (Hyodo et al., 2002) and we did not find any different results on the cyclic shear characteristics between the two different frequencies. Besides the test results of scoria being comparable to Toyoura sand, by using 0.05 Hz of axial loading frequency we can control the accuracy of stresses, displacement measurement and pore water pressure. In view of this, we considered that 0.05 Hz is an appropriate axial loading frequency value for this study. Axial loads were measured by a load cell with 2 kN capacity installed between top cap of pedestal and a piston in a cell and axial strains were monitored by a displacement transducer out of the cell. The electrical outputs from the load cell, displacement transducer and pore water pressure transducer were amplified and then recorded simultaneously by a computer.

The stress parameters used in the present study have been defined as follows:
The effective mean principal stress:

$$p' = (\sigma'_a + 2\sigma'_r)/3 \quad (1)$$

and the deviator stress:

$$q = \sigma'_a - \sigma'_r \quad (2)$$

in which σ'_a is axial effective stress and σ'_r is lateral effective stress (which is also defined as σ'_c or effective confining stress), respectively.
And to find the lateral effective stress or effective confining stress we used:

$$\sigma'_r = \sigma'_c = \mathrm{DP} + \Delta\sigma_m \quad (3)$$

where DP is the differential pressure between cell water pressure and the pore water pressure, and $\Delta\sigma_m$ is the stress correction for the force working in the membrane. The stress correction was calculated using the equation of ''Hoop tension theory'' by Henkel and Gilbert (1952).

$$\Delta\sigma_{\mathrm{m}} = -\frac{2tE_{\mathrm{m}}}{d}\,\varepsilon_{\mathrm{m}} \qquad (4)$$

in which t is membrane thickness, E_m is membrane Young's modulus, d is sample diameter and ε_m is the circumferential strain of membrane.

RESULTS

Isotropic Consolidation

Isotropic consolidation curves for the scoria samples used in the tests are shown in Fig. 4(a). The data included here was taken from volume change and consolidation stress measurements on all samples tested. The volume change of scoria was very small during consolidation, so that the change of void ratio during isotropic consolidation is very small. Result from some samples sieved before and after isotropic consolidation shows that there was no considerable particle crushing determined during isotropic consolidation, as shown by Fig. 4(b). Hyodo et al. (2002) investigated the monotonic and cyclic shear behaviour of Aio sand and showed considerable particle crushing was initiated at stresses greater than 3 MPa in isotropic consolidation.

Cyclic Stress-strain Relationships

Figures 5(a) and 6(a) show the relationship between cyclic deviator stress and axial strain for 100 kPa of confining pressure. These illustrate typical undrained cyclic behaviour of scoria. Here, the development of cyclic strains occurs in both compression and extension. Pore water pressure gradually increases with cyclic loading and shear strain increases dramatically when cyclic loading is generated near the failure line. Cyclic mobility occurs as the stress path cycles through zero effective confining pressure. As shown by Figs. 5(b) and 6(b), both curves reach the steady state with generating cyclic mobility as a common behaviour for usual sands such as Toyoura sand. While the results are not presented here, the same behaviour is seen for all samples tested in this study.

Figure 7 shows the relationships between the cyclic stress ratio $\sigma_d/2\sigma'_c$ (σ_d is cyclic deviator stress and $q=\sigma_d/2$) and the number of cycles N_c to cause liquefaction which is defined as strain double amplitude DA of 5%. Cyclic strength curves have been drawn for two series of relative density of scoria specimens. The solid and hollow squares show the results of loose and dense samples, respectively. Although there is a variation in the specimen density after the consolidation which is reconstituted, the liquefaction strength of scoria is not so much different.

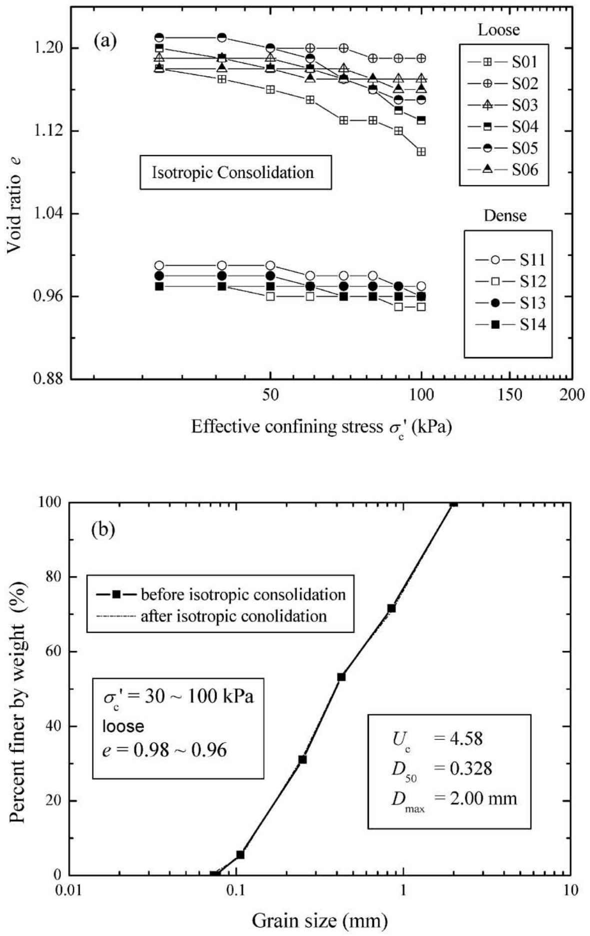

Fig. 4. Isotropic consolidation: (a) two series of scoria before cyclic loading applied and (b) grain size distribution before and after isotropic consolidation

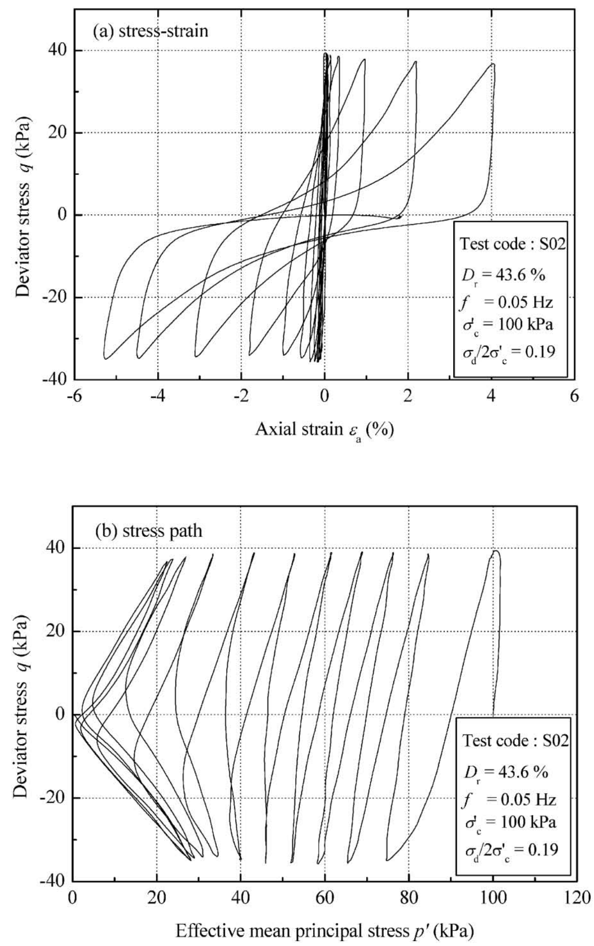

Fig. 5. Results of undrained cyclic triaxial tests on S02 test code of scoria: (a) stress-strain relationships and (b) stress path

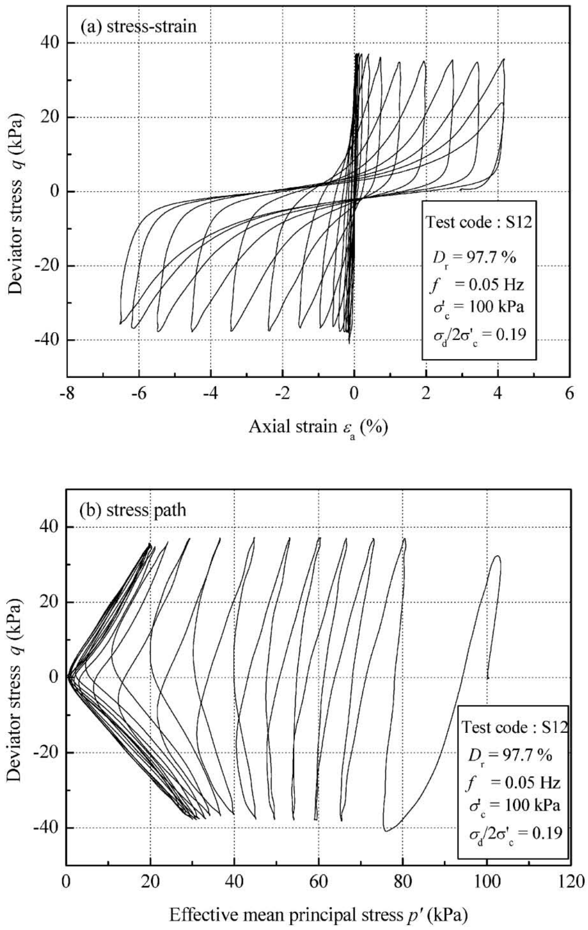

Fig. 6. Results of undrained cyclic triaxial tests on S12 test code of scoria: (a) stress-strain relationships and (b) stress path

Table 2. Comparing to other materials results from other authors

(1)	(2)	(3)	(4)	(5)	(6)	(7)
Authors	Material	G_s	e_{max}	e_{min}	U_c	D_{max} (mm)
Hatanaka et al. (1985)	Shirasu	2.41 ~ 2.50	1.060	0.790	8.9 ~ 16.3	10.00
Hyodo et al. (1998)	Toyoura	2.643	0.973	0.635	1.20	0.425
	Dogs Bay sand	2.723	2.451	1.621	1.92	0.85
Agustian and Goto (2008)	Scoria	2.722	1.407	0.956	4.580	2.00

(3) specific gravity
(4) maximum void ratio
(5) minimum void ratio
(6) uniformity coefficient
(7) maximum grain size

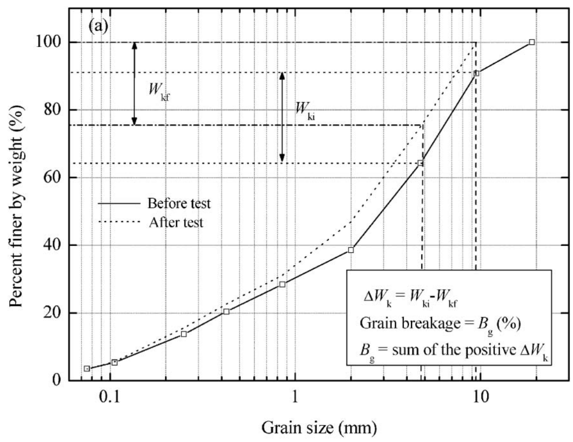

Fig. 8. Determination of grain breakage B_g (%) (Marsal, 1973)

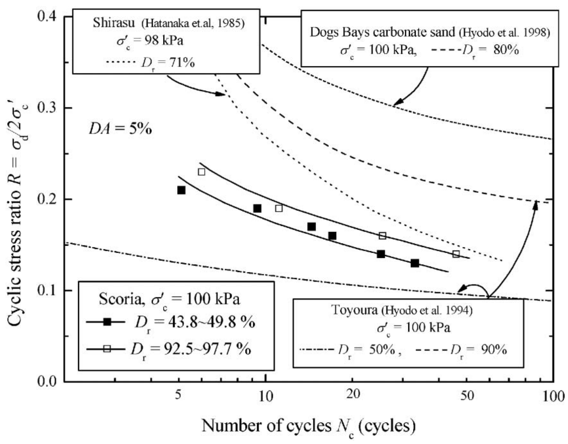

Fig. 7. Liquefaction strength of scoria material compared to other materials from previous studies

From the results, it was understood that the effect of relative density D_r on the cyclic shear strength of scoria material is small, in the range between 43.8 and 97.7 of D_r. The independency of dry density on shear strength was also shown by the results of triaxial compression tests in the previous study (Fig. 1(a)). This may be a typical strength characteristic of scoria material and needs some further investigations. Strength comparison between scoria and other materials (Table 2) presented here indicates that the liquefaction resistance of scoria seems to be lower than that from other materials in dense state.

Particle Crushing under Cyclic Shear Stresses

The method of evaluating grain breakage used in this study was originally proposed by Marsal (1973). In his pioneer work, Marsal performed a large triaxial test on the granitic-gneiss rockfill from Mica Dam to define a quantitative measure of grain breakage. Principally, grain breakage B_g is obtained by calculating the difference ΔW_k between percentage of the total sample contained in each grain size fraction before the test ΔW_{ki} and after the test ΔW_{kf}. The difference between the percentage of the total sample contained in each grain size fraction before and after the test is plotted versus the opening of the upper sieve corresponding to that fraction. The algebraic sum of this difference is zero. Then the grain breakage B_g is equal to the sum of the positive total differences, and expressed in percent (*see* Fig. 8).

$$\Delta W_k = \Delta W_{ki} - \Delta W_{kf} \tag{5}$$

and B_g is the total sum of positive ΔW_k.

The degree of grain breakage after cyclic loading was

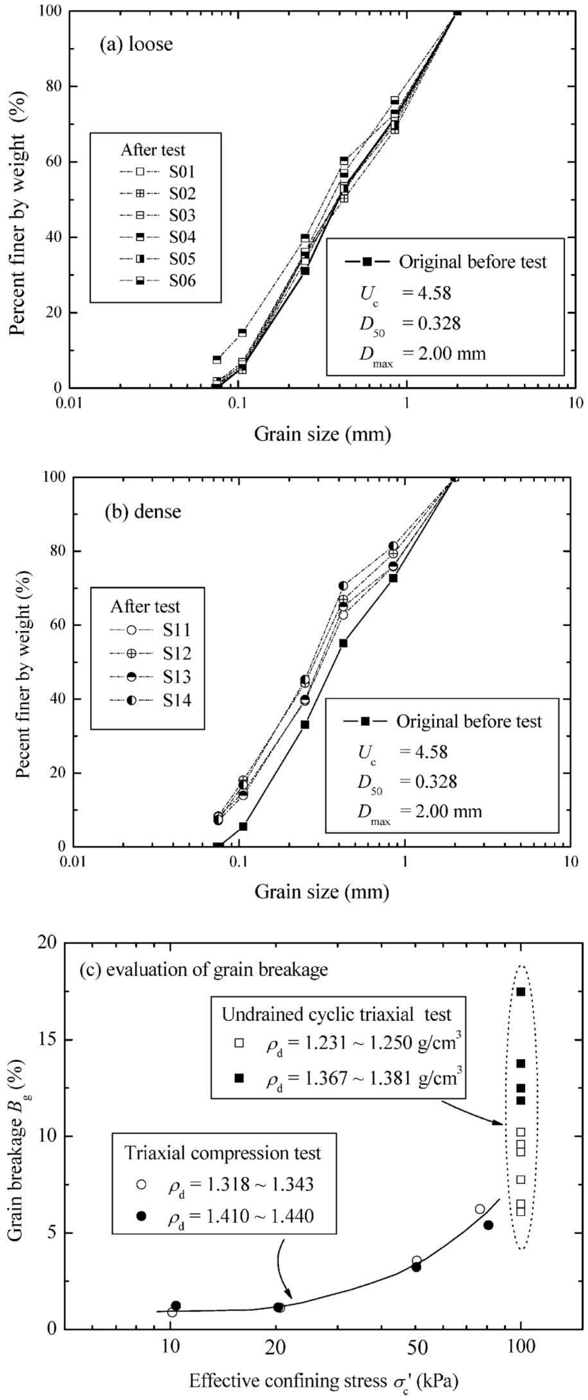

Fig. 9. Gain breakage of scoria samples: (a) grain size distribution before and after the tests of loose samples, (b) grain size distribution before and after the tests of dense samples and (c) calculation results compared to triaxial compression test

measured using the technique described above. Samples were cycled until about 10% double amplitude strain. Figures 9(a) and (b) are the grain size distributions of scoria before and after the cyclic shear test for loose and dense samples, respectively. The difference of grain size distribution before and after the tests on both loose and dense samples is clearly seen. The increment of fine content (75 μm or less) that confirmed after the tests, reach 8 % at maximum for dense samples and 7% for loose samples, indicate that particle breakage seems to occur significantly during the tests. The degree of grain breakage during cyclic shear stress is shown by Fig. 9(c). The figure also shows the grain breakage of scoria results from cyclic triaxial test as compared to those from monotonic triaxial compression test. Comparison results between monotonic and cyclic triaxial test on grain breakage due to shearing show that degree of grain breakage for cyclic triaxial test is relatively higher than from monotonic for a similar dry density.

CONCLUSIONS

In order to evaluate the characteristics of cyclic strength of scoria, undrained cyclic triaxial tests were performed on scoria with varying cyclic stress ratio. On the basis of the limited number of tests reported, even though there are several things difficult to explain and need some further investigations, the experiment has helped to elucidate the cyclic shear strength characteristics of reconstituted scoria whose characteristics have not been studied so much until present. The following conclusions were obtained:

1. The volume change of scoria was very small during consolidation, so that the change of void ratio during isotropic consolidation is very small. Results from some samples sieved before and after isotropic consolidation shows that there was no considerable particle crushing determined during isotropic consolidation.
2. Undrained cyclic behaviour between loose state and dense state of scoria is not very much different. Comparison results between scoria and other materials presented indicate that the liquefaction resistance of scoria seems to be lower than that from other materials in dense state.
3. While some scatters appear in the data, there was a significant amount of particle breakage after the cyclic test. The degree of grain breakage due to shearing results from cyclic triaxial test is relatively higher compared to monotonic triaxial test for a similar dry density.

REFERENCES

1) Agustian, Y. and Goto, S. (2008): Strength and deformation characteristics of scoria in triaxial compression at low confining stress, *Soils and Foundations*, **48**(1), 27–39.
2) Fukushima, S. and Tatsuoka, F. (1984): Strength and deformation characteristics of saturated sand at extremely low pressures, *Soils and Foundations*, **24**(4), 30–48.
3) Hatanaka, M., Sugimoto, M. and Suzuki. Y. (1985): Liquefaction resistance of two alluvial volcanic soils sampled by in situ freezing, *Soils and Foundations*, **25**(3), 49–63
4) Henkel, D. J. and Gilbert, G. C. (1952): The effect of rubber on the measured triaxial compression strength of clay samples, *Géotechnique*, **3**, 20–29.
5) Hossein, A. M. K. (2006): Blended cement and lightweight concrete using scoria: mix design, strength, durability and heat insulation characteristics, *International Journal of Physical Sciences*, **1**(1), 5–16.

6) Hyodo, M., Hyde, A. F. L. and Aramaki, N. (1998): Liquefaction of crushable soils, *Géotechnique*, **48**, 527–543.
7) Hyodo, M., Hyde, A. F. L., Aramaki, N. and Nakata, Y. (2002): Undrained monotonic and cyclic shear behaviour of sand under low and high confining stress, *Soils and Foundations*, **42**(3), 63–76.
8) Kusakabe, O., Maeda, Y., Ohuchi, M. and Hagiwara, T. (1991): Strength- deformation characteristics of an undisturbed scoria and effects of sample disturbance, *Proc. Japan Society of Civil Eng.*, (**439**/III–17), 69–77 (in Japanese).
9) Marsal, R. J. (1973): Mechanical properties of rockfill, *Embankment Dam Engineering*, Casagrande Volume, 109–199.
10) Miura, S., Yagi, K. and Asonuma, T. (2003): Deformation strength evaluation of crushable volcanic soils by laboratory and in-situ testing, *Soils and Foundations*, **43**(4), 47–57.
11) Sabtan, A. A. and Shehata, W. M. (2000): Evaluation of engineering properties of scoria in central Harrat Rahat, Saudi Arabia, *Bulletin of Engineering Geology and the Environment*, **59**(3), 219–225.